

Porous Graphene-Based Flexible On-Chip Microsupercapacitors Enabled by Chitosan Oligosaccharide Laser Lithograph

Huang, Qian Ming; Yang, Huiru; Wang, Shaogang; Zhang, Guoqi; French, Paddy; Ye, Huaiyu

DOI

[10.1109/NEMS60219.2024.10639907](https://doi.org/10.1109/NEMS60219.2024.10639907)

Publication date

2024

Document Version

Final published version

Published in

2024 IEEE 19th International Conference on Nano/Micro Engineered and Molecular Systems, NEMS 2024

Citation (APA)

Huang, Q. M., Yang, H., Wang, S., Zhang, G., French, P., & Ye, H. (2024). Porous Graphene-Based Flexible On-Chip Microsupercapacitors Enabled by Chitosan Oligosaccharide Laser Lithograph. In *2024 IEEE 19th International Conference on Nano/Micro Engineered and Molecular Systems, NEMS 2024* (2024 IEEE 19th International Conference on Nano/Micro Engineered and Molecular Systems, NEMS 2024). IEEE. <https://doi.org/10.1109/NEMS60219.2024.10639907>

Important note

To cite this publication, please use the final published version (if applicable). Please check the document version above.

Copyright

Other than for strictly personal use, it is not permitted to download, forward or distribute the text or part of it, without the consent of the author(s) and/or copyright holder(s), unless the work is under an open content license such as Creative Commons.

Takedown policy

Please contact us and provide details if you believe this document breaches copyrights. We will remove access to the work immediately and investigate your claim.

Green Open Access added to TU Delft Institutional Repository

'You share, we take care!' - Taverne project

<https://www.openaccess.nl/en/you-share-we-take-care>

Otherwise as indicated in the copyright section: the publisher is the copyright holder of this work and the author uses the Dutch legislation to make this work public.

Porous Graphene-Based Flexible On-Chip Microsupercapacitors Enabled by Chitosan Oligosaccharide Laser Lithograph

Qian-Ming Huang,^{†,‡} Huiru Yang,^{†,‡} Shaogang Wang,^{†,#} Guoqi Zhang,[#] Paddy French,[#] and Huaiyu Ye^{*,†,#}
*Email: h.ye@tudelft.nl

[†] School of Microelectronics, Southern University of Science and Technology, Shenzhen 518055, China.

[‡] Harbin Institute of Technology, Harbin 150001, China.

[#] Faculty of EEMCS, Delft University of Technology, 2628 CD Delft, The Netherlands.

Abstract—This research introduces a novel and convenient technology, chitosan oligosaccharide laser lithography (COSLL), enabling the creation of flexible laser-induced graphene (LIG) on-chip microsupercapacitors (MSCs) using environmentally friendly chitosan-class polymers for the first time. MSCs prepared through COSLL exhibit a significant areal capacitance exceeding 4 mF cm^{-2} , comparable to that of the polyimide-LIG-based counterparts. COSLL seamlessly integrates with the micro-nano thin-film process, allowing the capacitance of resulting LIG/Au MSCs to be further increased to about 8 mF cm^{-2} . Leveraging an eco-friendly biomass carbon source and featuring a convenient process flowchart, COSLL emerges as an appealing method for fabricating flexible LIG on-chip MSCs.

Keywords—laser-induced graphene, microsupercapacitor, chitosan oligosaccharide, laser lithograph

I. INTRODUCTION

laser-induced graphene (LIG) electrodes, created through direct laser writing (DLW) on polymer substrates, have found extensive applications in various flexible microsupercapacitors (MSCs) [1]. Remarkable strides have been taken in the realm of synthetic polymer-based LIG flexible electronics. In the pursuit of environmentally friendly alternatives, there is a growing interest in utilizing biomass carbon sources to fabricate LIGs for flexible MSCs [2]. Among these sources, chitosan stands out as a widely available biomass carbon source, known for its biocompatibility, biodegradability, and non-toxic properties [3]. Recent efforts have demonstrated the transformation of chitosan-based composites or derivatives into conductive LIGs, leading to breakthroughs in electrochemical sensors [4] and triboelectric nanogenerators [5]. However, a significant challenge arises with chitosan-based polymer thin films, as they exhibit high susceptibility to brittleness or deformation when exposed to slight variations in temperature, humidity, or mechanical stress. Consequently, despite these advancements, the application of chitosan-class polymer-derived LIG MSCs remains unexplored, primarily due to the formidable reliability challenges associated with these materials, as far as our current knowledge extends.

In this study, pioneering chitosan oligosaccharide laser lithography (COSLL) technology is introduced for LIG synthesis and reliable MSC preparation. In this process, chitosan oligosaccharide (COS) is blade-coated onto the heterogeneous engineering plastic films, forming a conformal double-layer structures. Subsequently, employing a simple one-step CO_2 laser treatment, the COS carbon source layer undergoes facile pyrolysis to yield meticulously crafted LIG interdigital electrodes, and the resulting film electrodes are securely bonded to the engineering polymer

substrate. After a further peeling-off process to remove the residual precursor, LIG electrodes can be packaged into desired on-chip MSCs, and the devices exhibit both high reliability and high performance. Herein, we report the COSLL method, the microscopic morphology of COS-derived LIG, and the electrochemical performance of the corresponding flexible on-chip MSCs.

II. RESULTS AND DISCUSSIONS

A. Chitosan Oligosaccharide Laser Lithography Process

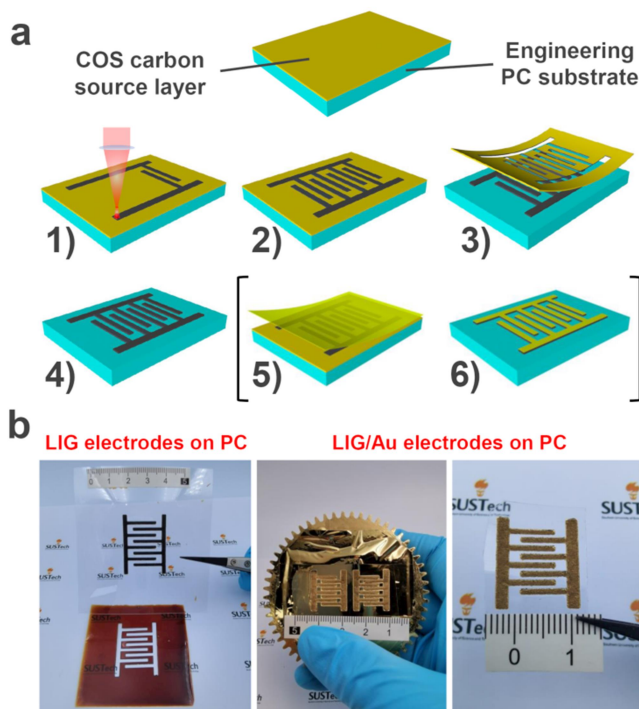


Figure 1. (a) Flowchart illustrating the COSLL process, mainly including blade-coating, laser engraving, and peeling-off, step 5–6: additional metal layer deposition before removal. (b) Laser-printed LIG interdigital electrodes on PC substrate alongside mechanically stripped COS/PVA residue film and Au-deposited LIG/Au composite interdigital electrodes on PC film.

The comprehensive process flow diagram for the COSLL method is depicted in Figure 1a. Initially, a uniformly mixed solution of COS and PVA was meticulously blade-coated onto the surface of the plastic polycarbonate (PC) substrate. This process resulted in the formation of a snug-fitting bilayer film structure through conformal contact. Given the remarkably high water solubility of COS, PVA was selected as the binder to achieve effective blade-coating without interfering in the subsequent LIG formation [6]. Subsequently, the conformal composite film underwent

exposure to a 10.6 μm CO_2 infrared laser. The COS/PVA layer was instantaneously pyrolyzed into LIG electrodes, precisely following the pre-designed interdigital shapes (Figure 1a, steps 1–2). The unexposed and dry transferable residual COS/PVA was then efficiently removed through a straightforward or water-assisted mechanical peeling-off process, leaving only the bare LIG electrodes adhered to the plastic substrate (Figure 1a, steps 3–4). It is worth noting that the water-assisted peeling-off is more efficient and lossless, especially for high-precision patterning with smaller critical dimensions, but requires an additional post-drying treatment. Moreover, COSLL seamlessly integrates with the film deposition process of the Complementary Metal–Oxide–Semiconductor (CMOS) or Micro–Electro–Mechanical System (MEMS) processes (Figure 1a, steps 5–6). With the metal deposition before the removal step, the metal film will be deposited onto the surface of the interdigital structure and COS/PVA serves as a barrier layer at this point.

As depicted in Figure 1b, the as-prepared COS/PVA film was attached to the surface of a PC substrate. Through a single CO_2 laser engraving step, dark red COS/PVA transforms into black LIGs, and after the removal process, interdigital LIG electrodes on the PC film are obtained, with unexposed residues easily stripped off without causing damage. Importantly, COSLL allows for the realization of arbitrary LIG patterns on the PC substrate. However, sufficient laser energy is imperative for effective thermal fusion connection; otherwise, the formed LIGs may remain in the carbon source layer. Figure 1b also showcases the LIG/Au composite electrode obtained through magnetron sputtering, which is beneficial for enhancing the electrical conductivity of the LIG network. Thanks to the convenience afforded by COSLL, interdigitated LIG electrodes can be easily prepared in batches, laying the foundation for the modular integration of MSC devices.

The COSLL method stands out for its ability to transform arbitrarily designed graphics into tangible conductive LIG products on heterogeneous engineered polymer substrates. This capability aligns with the standard definition of a lithography process. When compared to traditional lithography (Figure 2), COSLL boasts the advantage of not necessitating additional masks, development steps, or metal layer depositions. This streamlined approach enhances the convenience of preparing flexible on-chip devices, including MSCs. Notably, as previously mentioned, COS can also serve as a dry transferable photoresist, facilitating additional CMOS or MEMS-based metal film deposition processes. This application can be harnessed to craft LIG-metal composite electrodes and MSCs with superior performance. While DLW represents the simplest among the three technologies (Figure 2), it cannot directly fabricate reliable devices based on carbon source substrates with weak mechanical properties, such as chitosan-based materials. In contrast, COSLL excels by enabling the in-situ transfer of generated LIG to a heterogeneous target substrate through the establishment of a double-layer structure comprising a carbon source layer and a support layer. This unique feature contributes to the creation of highly reliable devices from chitosan-based precursors. In essence, the eco-friendliness inherent in the core COS carbon precursor, combined with the simplicity of the processing steps, renders COSLL an exceedingly attractive technology for the fabrication of LIG MSCs and other advanced devices.

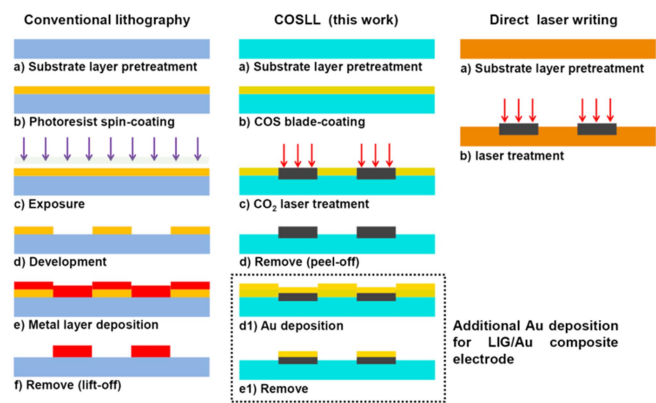


Figure 2. Comparison of flowcharts for conventional lithography, direct laser writing, and COSLL method of this work.

B. Microscopic Morphology of Laser-Induced Graphene

The microscopic morphology of COS-derived LIGs were subject to thorough investigation. Scanning electron microscopy (SEM) images of LIG (obtained at a laser power of 8.5%, LIG85) reveal the presence of distinctive coral-like hierarchical porous structures (Figure 3a), resembling those observed in pure COS-derived LIGs [5]. Further insights from high-resolution SEM photos (Figures 3b and 3c) expose the intricate composition of the coral-like miniature body, comprised of lamellar thin layers and profoundly stereoscopic macropore architectures. Close to the substrate's inner surface, a discernible fiber structure becomes apparent. The dense bubble macropores likely result from the release of gaseous products (CO , H_2O , CO_2 , etc.) during the drastic decomposition of precursors [7], while the fibrous structure may emerge from the mixing of cooled LIGs and the molten pool of the substratum. It is worth noting that a previous study indicated that the decomposition of the binder PVA does not yield carbon materials [6]; however, the gaseous products may still play an important role in fostering the creation of porous configurations. Transmission electron microscopy (TEM) images further unveil the thin-layer structure and multi-scale nanopore distributions of LIG sample. As illustrated in Figure 3d, the randomly stacked sheet carbon structures exhibit evident macropores with smooth edges, while numerous clustered meso- and micropores become apparent in high-resolution TEM (Figure 3e). These interleaved carbon structures and the randomly distributed nanopore networks of varying sizes reflect the intricate reaction kinetics during laser pyrolysis. The intricate porous architectures of LIGs imply a wealth of electrochemically active sites, providing ample channels for electrolyte diffusion and ion transport. This intricacy significantly contributes to the enhanced electrochemical performance of MSCs. A more detailed high-resolution TEM image of LIG (Figure 3f) revealed clear strip bands, with each strip representing a single-layer graphene. This phenomenon is often induced by thermal stress, leading to edge bending after laser pyrolysis [7]. A characteristic d -space of ~ 3.4 Å, measured from adjacent fringes, aligned with the interplanar spacing of neighboring (002) crystalline planes of graphitic carbons [8]. The selected area electron diffraction (SAED) pattern (inset of Figure 3f) presented two evident rings indexed to (002) and (001) peaks, indicating the presence of polycrystalline structures and demonstrating the graphitic lattice of LIG. In summary, these analyses underscore that the desired 3D hierarchical porous LIG

materials can be successfully obtained on PC substrates using the COSLL technique at a proper laser power.

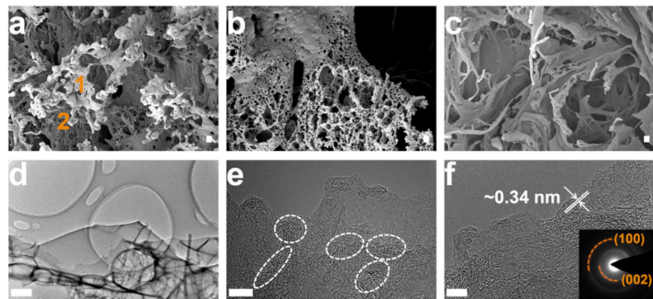


Figure 3. (a) SEM image of LIG obtained at a laser power of 8.5%, featuring a scale bar of 10 μm . (b, c) High-resolution SEM images captured from site 1 and site 2 of (a), respectively, showcasing scale bars of 1 μm . (d) TEM image of LIG, accompanied by a scale bar of 1 μm . (e, f) High-resolution TEM images of LIG, highlighting scale bars of 10 and 5 nm, respectively. Oval marks in (e) draw attention to the clustered nanopores, while the inset in (f) reveals the SAED pattern.

C. Electrochemical Performance of Microsupercapacitors

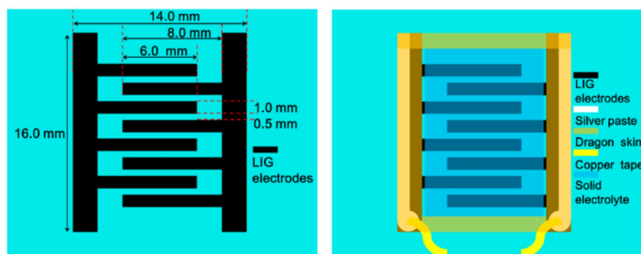


Figure 4. Dimensions of as-fabricated LIG eight-interdigitated electrodes and package structures of MSCs.

Leveraging the COSLL technique, eight-folded LIG (obtained at a laser power of 7.5%, also named LIG75) and LIG/Au in-plane interdigital electrodes with a total area of 0.48 cm^2 were fabricated on the PC film. Subsequently, these electrodes were integrated into all-solid on-chip MSCs employing PVA/ H_2SO_4 gel electrolytes (Figure 4) and the electrochemical performance of the resulting MSCs is elucidated. Galvanostatic charge-discharge (GCD) tests showcase that, in a complete charge and discharge cycle, both LIG and LIG/Au electrodes exhibit symmetrical GCD curves (Figures 5a and 5b), indicative of robust electric double-layer capacitor (EDLC) behavior and excellent Coulomb efficiency. As depicted in Figure 5c, LIG electrodes achieve a maximum areal capacitance of 4.3 mF cm^{-2} at a current density of 0.01 mA cm^{-2} , and this peak value is comparable to or higher than that of previously developed on-chip MSCs based on LIG interdigitated electrodes derived from various carbonaceous precursors, such as classical polyimide [7], graphite oxide [9], lignin [6], and metal-organic framework [10]. The plots of areal capacitance as a function of current density in Figure 5c provide a more comprehensive view of the impact of Au decoration. Within the current density range from 2 to 0.05 mA cm^{-2} , constrained by the porous LIG itself, the areal capacitance of LIG/Au MSCs exhibits an almost identical trend to that of its LIG counterparts. Only as the current density further decreases (0.02 to 0.01 mA cm^{-2}), does the areal capacitance of the LIG/Au device differentially increase, reaching a high performance of 7.9 mF cm^{-2} at 0.01 mA cm^{-2} , approximately twice that of LIG (4.3 mF cm^{-2}). The main reason for this phenomenon is that gold can only be deposited on the surface layer of 3D LIG architectures.

Therefore, only at lower current densities can the Au coating overcome the transmission limitations of the LIG network and enhance the interface properties of the electrolyte and electrode, thereby improving charge transfer efficiency and capacitance. In addition to improving areal capacitance, the gold coating significantly reduces the equivalent series resistance of the MSCs (Figure 5d), enhancing the maximum power point for external loads.

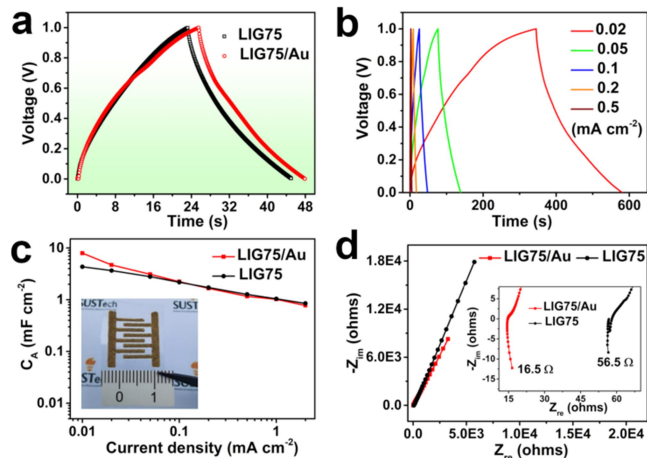


Figure 5. (a) GCD curves of LIG MSC and LIG/Au MSC, measured at a current density of 0.1 mA cm^{-2} . (b) GCD profiles of LIG/Au MSC measured at different current densities. (c) Areal capacitance comparison between LIG and LIG/Au MSCs obtained from GCD tests. (d) Nyquist plots and zoomed-in Nyquist plots (inset) for LIG and LIG/Au MSCs.

III. CONCLUSION

In conclusion, based on eco-friendly chitosan-class biomass material, we have successfully developed a convenient COSLL technology for the preparation of hierarchically porous LIG electrodes and flexible on-chip MSCs. LIG MSCs prepared by COSLL demonstrate substantial areal capacitance exceeding 4 mF cm^{-2} , comparable to PI-derived LIG MSCs. With an additional CMOS and MEMS-compatible film deposition process, the composite LIG/Au electrode can further elevate the areal capacitance to around 8 mF cm^{-2} . This work provides a new approach for the fabrication of flexible on-chip LIG MSCs.

ACKNOWLEDGMENT

This work was supported by the National Key R&D Program of China (2018YFE0204600), the Shenzhen Fundamental Research Program (JCYJ20200109140822796), Joint Lab of Advanced Situation Awareness, Joint Lab of Advanced Packaging Technology, and Joint Lab of Advanced Packaging and Testing Technology of Integrated Circuits.

REFERENCES

- [1] T. S. D. Le *et al.*, "Recent Advances in Laser-Induced Graphene: Mechanism, Fabrication, Properties, and Applications in Flexible Electronics," *Advanced Functional Materials*, p. 2205158, 2022.
- [2] A. C. Bressi *et al.*, "Bioderived Laser-Induced Graphene for Sensors and Supercapacitors," *ACS Applied Materials & Interfaces*, vol. 15, no. 30, pp. 35788-35814, 2023.
- [3] F. G. Torres, and G. E. De-la-Torre, "Polysaccharide-based triboelectric nanogenerators: A review," *Carbohydrate Polymers* vol. 251, p. 117055, 2021.
- [4] C. Larrigy *et al.*, "Porous 3D Graphene from Sustainable Materials: Laser Graphitization of Chitosan," *Adv. Mater. Technol.*, vol. 8, p. 2201228, 2023.

- [5] Q.-M. Huang *et al.*, "Laser-Induced Graphene Formation on Chitosan Derivatives toward Ecofriendly Electronics," *ACS Applied Nano Materials*, vol. 6, no. 12, pp. 10453-10465, 2023.
- [6] W. Zhang *et al.*, "Lignin Laser Lithography: A Direct-Write Method for Fabricating 3D Graphene Electrodes for Microsupercapacitors," *Advanced Energy Materials*, vol. 8, no. 27, p. 1801840, 2018.
- [7] J. Lin *et al.*, "Laser-induced porous graphene films from commercial polymers," *Nature Communications*, vol. 5, p. 5714, 2014.
- [8] G. Yang *et al.*, "Structure of graphene and its disorders: a review," *Sci Technol Adv Mater*, vol. 19, no. 1, pp. 613-648, 2018.
- [9] M. F. El-Kady, and R. B. Kaner, "Scalable fabrication of high-power graphene micro-supercapacitors for flexible and on-chip energy storage," *Nat Commun*, vol. 4, p. 1475, 2013.
- [10] W. Zhang *et al.*, "Laser-Assisted Printing of Electrodes Using Metal-Organic Frameworks for Micro-Supercapacitors," *Advanced Functional Materials*, vol. 31, no. 14, p. 2009057, 2021.